Predicting the optimal process window for the coating of single-crystalline organic films with mobilities exceeding 7 cm^2/Vs.

Robby Janneck*[a,b], Federico Vercesi[a], Paul Heremans[a,b], Jan Genoe[a,b] and Cedric Rolin[a]
[a]IMEC, Kapeldreef 75, Leuven B-3001, Belgium;
[b]Dept. Elektrotechniek – ESAT, KU Leuven, Kasteelpark Arenberg 10, Leuven B-3001, Belgium

ABSTRACT

Organic thin film transistors (OTFTs) based on single crystalline thin films of organic semiconductors have seen considerable development in the recent years. The most successful method for the fabrication of single crystalline films are solution-based meniscus guided coating techniques such as dip-coating, solution shearing or zone casting. These up-scalable methods enable rapid and efficient film formation without additional processing steps. The single-crystalline film quality is strongly dependent on solvent choice, substrate temperature and coating speed. So far, however, process optimization has been conducted by trial and error methods, involving, for example, the variation of coating speeds over several orders of magnitude. Through a systematic study of solvent phase change dynamics in the meniscus region, we develop a theoretical framework that links the optimal coating speed to the solvent choice and the substrate temperature. In this way, we can accurately predict an optimal processing window, enabling fast process optimization. Our approach is verified through systematic OTFT fabrication based on films grown with different semiconductors, solvents and substrate temperatures. The use of best predicted coating speeds delivers state of the art devices. In the case of C_8BTBT, OTFTs show well-behaved characteristics with mobilities up to 7 cm^2/Vs and onset voltages close to 0 V. Our approach also explains well optimal recipes published in the literature. This route considerably accelerates parameter screening for all meniscus guided coating techniques and unveils the physics of single crystalline film formation.

Keywords: meniscus-guided coating, zone-casting, single crystal, field-effect mobility, OTFT, C8-BTBT, TIPS-Pentacene

1. INTRODUCTION

Organic thin film transistors are promising candidates for low-cost, large-area electronic applications on flexible substrates[1–3]. The latest generation of organic semiconductors already achieves mobilities surpassing those of amorphous silicon thin film transistors (TFTs), which are commonly used in today's flat panel displays[3–5]. Due to their ability to realize efficient charge transport and thereby achieve high performance, single-crystalline thin films are the ultimate morphology for the semiconductor layer[6–9]. The most advanced techniques to fabricate crystalline thin films on amorphous dielectric substrates are solution-based meniscus guided coating (MGC) techniques, such as zone casting[10–14], dip- coating[15,16], solution shearing[17–20], hollow pen writing[9] or modified edge casting[21]. They all rely on a unidirectional motion of a drop of solution relative to the substrate.

In MGC techniques, the coating speed, substrate temperature and solvent choice has a large influence on the film morphology and hence on the electrical characteristics[14,16,22,23]. Previous studies have already shown that there exists an optimized processing speed for different combinations of solvent and substrate temperature[13–16]. This process window is, however, typically determined by a trial and error method, involving the variation of the coating speed over several orders of magnitude. Hence these studies are very specific to a given set of solvent choice and substrate temperature. Changing the solvent and/or the substrate temperature requires another trial and error approach to redefine the optimum processing window. To speed up process optimization and enable an easy transfer to different material systems and coating techniques, a model that predicts the process window is therefore highly desirable.

*robby.janneck@imec.be; phone: +32 16 28 81 46; http://www.eposcrystalli.eu/

Organic Field-Effect Transistors XV, edited by Iain McCulloch, Oana D. Jurchescu,
Proc. of SPIE Vol. 9943, 99430X · © 2016 SPIE · CCC code: 0277-786X/16/$18
doi: 10.1117/12.2235342

Here we develop a simple but versatile model that can accurately predict the process window for MGC techniques working in the evaporative (slow coating speeds) regime[24]. We first use edge casting experiments to measure the evaporation speed of menisci of common pure organic solvents at various temperatures. These evaporation speeds predict the coating speed for each solvent-temperature combination. Next, we develop a theoretical framework that captures the edge-casting results[14]. This model accurately predicts the coating speed for almost any solvent and substrate temperature combination. We show that this model explains well optimal recipes published in the literature that were developed through trial and error approaches. Finally, the predictive power of the model is validated through the fabrication of single crystalline films of 2,7-Dioctyl[1]benzothieno[3,2-b][1]benzothiophene (C_8-BTBT) using the zone-casting method. Devices based on these films present state of the art results with mobilities surpassing 7 cm^2/Vs when the active layer is grown at the best predicted coating speed.

2. EXPERIMENTAL PROCEDURE

2.1 Materials

We used highly doped silicon wafers with a 125 nm thick thermally grown SiO_2 layer as substrates. This provided the common gate and dielectric stack for the OTFT devices. The substrates were treated with a self-assembled monolayer (trichloro(phenethyl)silane; PETS) to increase the wettability of the solutions on the substrate. All solvents as well as PETS were purchased from Sigma Aldrich and were used as received. We used the commercially available semiconductor C_8-BTBT (supplied by Nippon Kayaku Co.) for film fabrication. Solutions were prepared in different solvents with a concentration of 0.25 wt%.

2.2 Experimental setup

We performed zone-casting experiments on a homebuilt slot-die coater (Fig. 1A) similar to the system used by Tracz and Pisula[10,11]. The slot-die coater head is fixed at a distance of 250 µm above the substrate. After injecting the initial solution to form an initial drop between the zone casting blade and the substrate, the meniscus shape was maintained by an automated solution supply. The substrate is translated by a stepper motor at speeds ranging from few µm/s to several hundred µm/s. The use of small translation speeds result in negligible shearing forces and therefore the contact angle can be considered to be static, resulting in a similar meniscus shape for different speeds.

Edge casting experiments were conducted in a similar fashion as previously described by Uemura et al.[25] on a sample kept in a horizontal position (Fig. 1B). This experiment was used to measure the evaporation times of pure solvents. We used a Dino-Lite microscope to record videos of the receding meniscus. The receding times over known distances were used to calculate the receding speeds for the solvents at various temperatures.

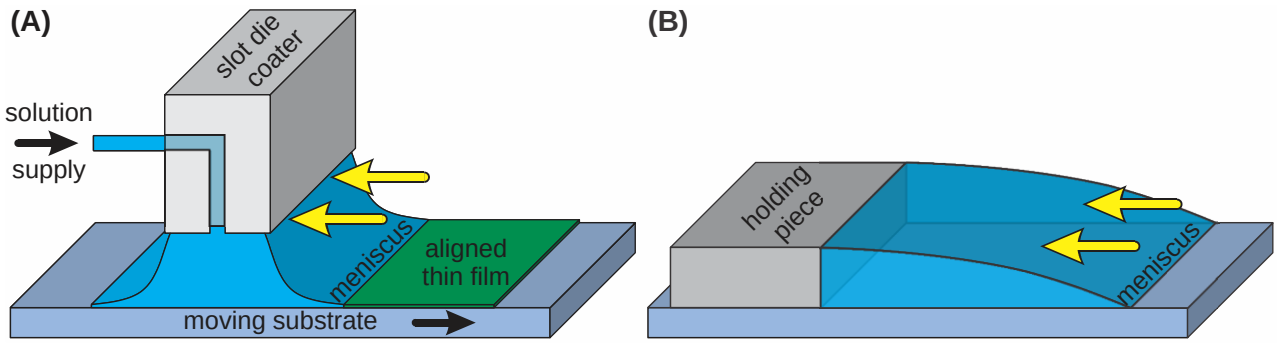

Figure 1: Experimental setup. Schematic representation of (A) the zone casting setup and (B) the edge casting experiment. Yellow arrows indicate the relative movement of the meniscus with respect to the substrate, indicating the similarity between the setups. Although the curvature of the drop is opposite between the two setups, the contact angle at the tip of the meniscus remains the same for identical solution, substrate and temperature[14].

2.3 Film characterization

Film morphology was characterized by AFM studies using a Bruker dimension edge AFM tool and polarized optical light microscopy (PLM) using an Olympus AX70 microscope. The PLM images are typically used to check long-range crystal orientation, while the AFM studies give further insight in the microscopic film morphology.

The most probable final application for these films is the fabrication of circuits based on many transistors. Hence we fabricated OTFTs in order to assess the electrical quality of our films and compare different processing parameters. Au contacts were vacuum evaporated through a shadow mask to form source and drain contacts. The channel length and width were 240 μm and 1900 μm, respectively. The dimensions defined by the electrode were used as the effective transistor channel dimensions for result analysis. Any reduction of the real channel width by void formation or ribbon-like growth in the films was not accounted for. To ensure proper electrical behavior, the samples were subsequently annealed for 40 hours in a glovebox filled with nitrogen. Measurements were performed using an Agilent Agt1500 in dry air. Field-effect mobilities were evaluated in the saturation regime by conventional transconductance analysis. The proper functioning of circuits requires high performance and low spread of the TFT characteristics. Therefore, we fabricated a total of 50 OTFTs for each condition and compared their average mobilities as a means to assess film quality.

3. RESULTS AND DISCUSSION

3.1 Optimization using the conventional trial and error method

We prepared single crystalline layers by a zone-casting method similar to the designs by Tracz and Pisula[10,11]. We used the organic semiconductor C_8-BTBT in heptane, as this combination has shown to give high mobility devices with band-like transport using edge casting for film formation[25–27]. In order to find the optimal processing speed, we initially performed the typical trial and error method typically seen in literature[13,15,16]. We fabricated films at coating speeds varying over an order of magnitude, ranging from 12.5 μm/s up to 125 μm/s.

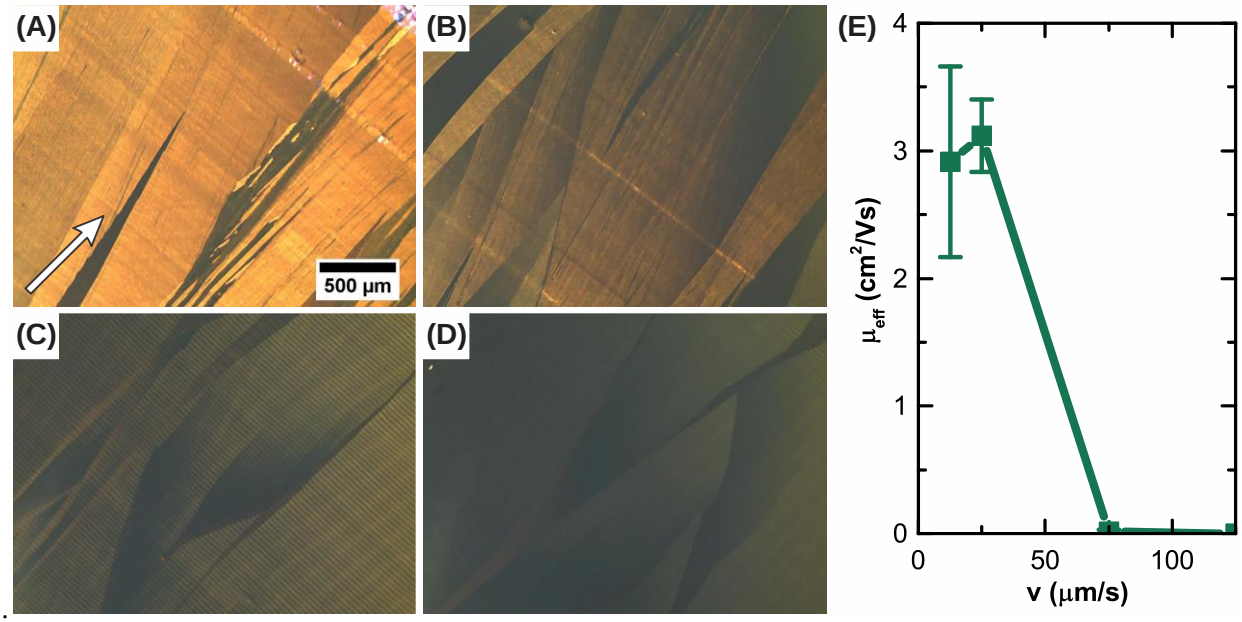

Figure 2: Optimization by the conventional trial and error method. PLM images of zone-casted C_8-BTBT films at speeds of 12.5 μm/s (A), 25 μm/s (B), 75 μm/s (C) and 125 μm/s (D) in heptane at room temperature. The white arrow indicates the direction of coating and is the same for all the images. (E) Effective hole mobility as a function of coating speed[14].

We used PLM to study the film morphology of the films formed at different coating speeds (Fig. 1A-D). In all cases, PLM reveals thin films with mm-sized single crystalline domains that are elongated along the translation direction. All images were taken with the same light exposure, hence darker images correspond to thinner films. Therefore it is

evident, that increasing coating speeds thins down the crystalline layers. AFM analysis confirmed this, as the thickness decreased from ~30nm at the slowest speed to around 5nm at the fastest coating speed. Furthermore the AFM study revealed, that the films actually grow in a ribbon-like fashion as was observed for different semiconductors beforehand[13–16]. The two slowest speeds result in well-interconnected ribbons that grow parallel to the coating direction. At larger coating speeds, these ribbons tend to narrow down and eventually form discontinuous islands. Hence there seems to be an optimum processing window at rather slow processing speeds.

Next, we fabricated OTFT arrays on top of these layers. For comparison reasons, we accounted for device spread by averaging the extracted mobility values over 50 different devices. The evolution of the electrical performance with coating speeds coincides well with the observation from the morphology analyses (Fig. 1E). Lower coating speeds result in the best performance, while higher coating speeds give orders of magnitude lower mobilities. Hence, as can be expected, thin and poorly connected ribbons or islands in the single crystalline domains result in only very few conductive paths and therefore low electrical performance. Moreover it can be seen, that the effective mobility values at the slowest tested speed (12.5 µm/s) show the highest statistical spread. One likely reason is the larger height deviation within the layer and therefore larger contact resistance variation. Moreover, at the slowest speed, aggregates are scattered all over the sample, as can be seen in the top right corner of Fig. 1A. These originate from precipitation of crystallites in the solution at slow speeds. Likely, the solvent is evaporating faster than the substrate is moving and the supply of solution is adapted to compensate this loss. This leads to a rise in organic solute concentration in the solution, especially in the meniscus region where evaporation is the strongest. Once the supersaturation point is reached, homogeneous nucleation and thereby crystal growth take place directly in the solution. These crystallites then deposit randomly over the whole sample. Therefore, we assume that the optimal processing window for heptane at room temperature is around 25 µm/s.

3.2 Edge casting experiments as a means to find the optimal processing speeds

It is well known, that the growth of a single crystalline thin film by a MGC technique results from is a complex physical process involving various different parameters. Especially the semiconductor, solvent, temperature and coating speed have a major influence on electrical characteristics of the thin films[13,14,16,22,23]. Nevertheless, previous studies have shown that there exist clear processing windows for the coating speed which are largely dependent on the solvent and temperature used[13–16]. Finding this processing window for different solvent-temperature combinations is typically done by a trial and error approach. However, as shown in the previous section, it is very time- and resource-consuming to fabricate OTFT devices for each combination of substrate temperature and solvent choice. Hence, we propose in this work a different, predictive approach.

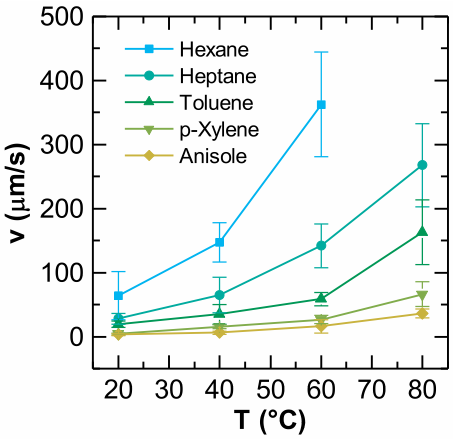

Figure 3: Edge casting results to determine processing speeds for common solvents and temperatures. Meniscus front evaporation speed of five pure solvents during an edge casting experiment at four different substrate temperatures.

MGC techniques rely on the unidirectional displacement of a solution drop across the surface of a substrate. The meniscus at the receding front is a region where the solvent readily evaporates. This results in the precipitation of the organic molecules which attach to the crystalline front already formed in the dried region. The edge casting method is a simple form of MGC where the unidirectional movement of the meniscus is solely governed by evaporation. Even though this technique is not optimal for large area coatings due to the limited area covered and the large transient

regions, this method uses no shearing forces and the freely moving meniscus front recedes at an equilibrium speed across the substrate that is only decided by evaporation dynamics. Measuring this speed enables a prediction of the optimal processing speed for other, more complex, MGC techniques due to their inherent similarities.

The receding speed of the meniscus front is mainly governed by the solvent and substrate temperature used. Even though the organic solute can have an influence on film morphology and electrical characteristics of the crystalline layer, it has been shown beforehand that, for a given solvent and temperature combination, the organic semiconductor only has a negligibly influence on the optimal processing speed[14,16]. Moreover the concentration of the solute in solution is typically in the order of 1 wt% or less. We therefore use the edge-casting of pure solvents to measure the receding speed of the meniscus. We show afterwards that this value provides a valid estimate for the optimal coating speed.

We measured the receding speeds of five different solvents at substrate temperatures of 20°C, 40°C, 60°C and 80°C (Fig. 3). As can be expected, rising substrate temperatures lead to faster receding speeds. This trend is visible for all the solvents tested. Furthermore higher boiling point solvents lead to slower evaporation rates, as the inter-molecular forces are stronger and hence the molecules are less likely to evaporate. We show next how these raw results can be interpolated and generalized to many solvents and substrate temperatures.

3.3 Developing a model to predict the optimal processing speeds

Even though the receding meniscus speeds measured in Fig. 3 could be directly exploited to speed up process optimization, it still requires an experiment for every combination of solvent and substrate temperature. Hence, a model that predicts the processing conditions for any combination of substrate temperature and solvent is desirable. When analyzing the data in Fig. 3, it becomes apparent that there is an exponential relationship between the evaporation speed of the meniscus and the temperature at the substrate (Fig. 4A). This temperature dependence is principally due to the activation energy needed for the solvent to evaporate, as described by the Arrhenius equation. This simple relationship allows the extraction of the evaporation speed and hence the optimal coating speed for the MGC technique at any temperature for all the solvents used in the edge casting experiment.

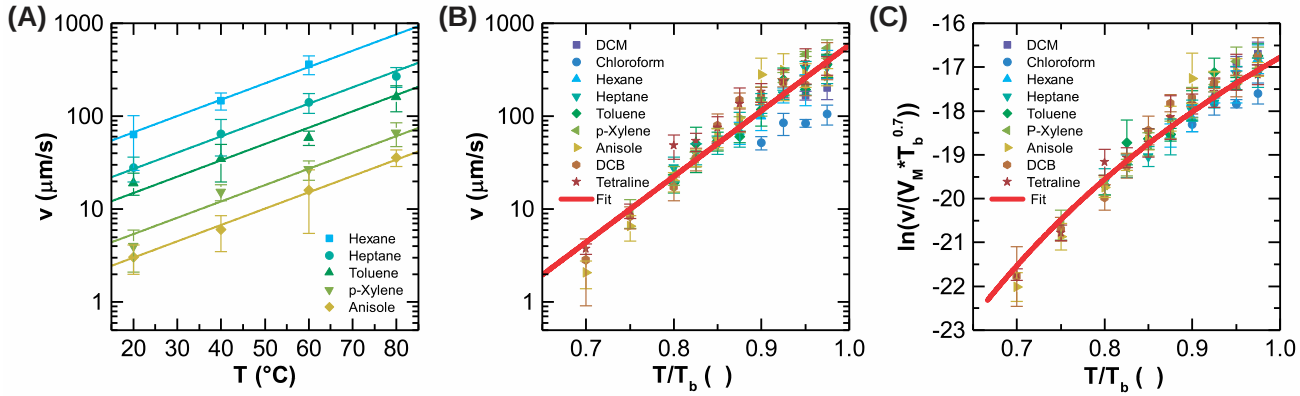

Figure 4: Edge casting experiments to predict the optimal coating speeds for a broad temperature range and a wide array of solvents. (A) Meniscus front evaporation speed of five pure solvents during edge casting experiments as a function of substrate temperature. (B) Meniscus front evaporation speed of nine pure solvents during an edge casting experiment as a function of temperature percentage of the respective boiling point of the solvent. (C) Same data as in (B), but replotted to allow a fitting parameter extraction for the theoretical framework given in the text[14].

Furthermore, the evaporation speed decreases with increasing boiling point. When normalizing the substrate temperature according to the respective boiling point of each solvent in Fig. 4B, we noticed a remarkable convergence of the data points along a single line. To check if this relationship between boiling point and evaporation speed is true for a broad range of substrate temperatures and solvents we performed edge casting experiments with nine different organic solvents with boiling points ranging from 40°C to 206°C. The edge casting experiments were performed at substrate temperatures ranging from 70% up to 97.5% relative to the respective boiling point of the solvents. As for the previous experiments, there is a remarkable convergence of most of the solvent curves when plotting the evaporation front speed as a function of T/T_b (Fig. 4B). The linear fit gives a good estimation of the evaporation speed for eight of the nine solvents with the measured values varying slightly around the fitted curve. However the fit always overestimates the evaporation speed for chloroform by about half an order of magnitude. Hence a model which takes more solvent

parameters into account than just the boiling point is required to accurately estimate the evaporation speed for any random choice of solvent and substrate temperature.

We have previously developed a physical model, taking into account the Clausius-Clapeyron relationship, the fluid dynamics of receding sessile drops, Trouton's rule and standard thermodynamic equations assuming that all solvent vapors behave as ideal gasses[14]. This model only requires knowledge of the solvent boiling point T_b, the solvent density ρ and molar mass MM as well as the substrate temperature T in order to predict the pure solvent meniscus receding speed v[14]:

$$v = 1870\,\mu m/s \cdot \frac{MM}{\rho} \cdot T^{0.7} \cdot \exp\left(-10.5 \cdot \frac{T_b}{T}\right). \quad (1)$$

As can be seen in Fig. 4C, all solvent curves plotted according to the model show a remarkable convergence and Eq. 1 gives a good fit for all of the tested solvents with a R^2 = 94%., In consequence, this model provides a good and generic estimation of the evaporation speed of pure solvent systems. It predicts meniscus receding speeds for a broad range of solvents and substrate temperatures, thereby providing an estimate for a successful processing window for the coating speed.

To verify this formula, we performed a COMSOL numerical simulation of the evaporation dynamics of a droplet of water in a two-dimensional edge casting geometry as depicted in the inset of Fig. 5A. We choose water as the evaporating liquid, as its characteristics are very well documented in literature. As seen in Fig. 5A we obtain a good match between our physical model in Eq. 1 and parameterized for water and the numerical calculations.

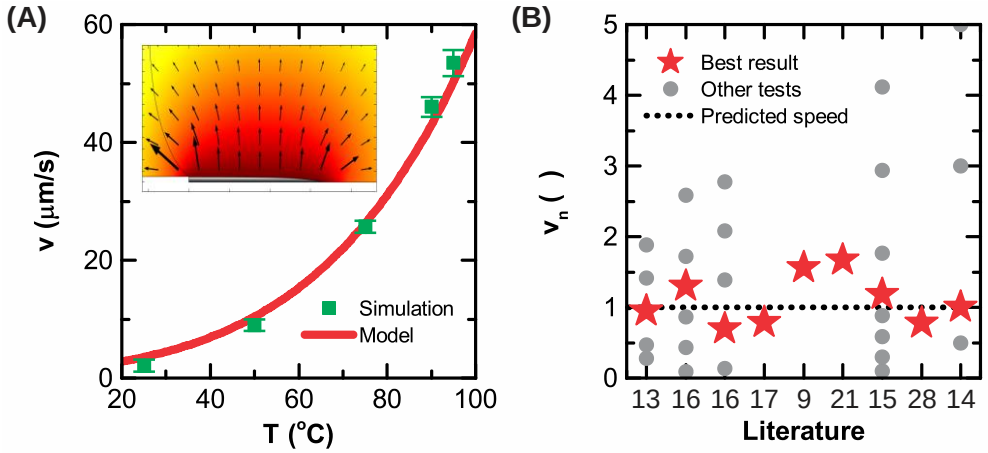

Figure 5: Verification of the predictive model by simulation and experimental results. (A) Velocity of the drying meniscus front as a function of T calculated by our model (red line) as well as by a COMSOL simulation (green squares). Inset shows the geometry of the edge casting model used in the numerical simulation. The color indicates the vapor concentration in the air surrounding the liquid meniscus. The arrows show the direction and intensity of the diffusive vapor flux away from the liquid[14]. (B) Comparison of the optimal coating speed predicted by our model with experimental results in literature[9,13–17,21,28].

Furthermore we compare our predicted speeds with experimental coating speeds in the literature, with the speeds optimized by a trial and error method. In the investigated papers we find a very good match between the reported coating speeds and the speeds predicted by our model. When normalizing the coating speed ($v_n = v_{Experiment} / v_{Model}$) we find that the best reported coating speeds in literature are always close to the predicted speed of our model. We looked at five different MGC techniques, seven different solvent systems, as well as six different organic semiconductors in a total of eight different papers[9,13–17,21,28]. The wide variety of MGC techniques, solvents and semiconductors employed in these studies show the broad applicability of our model to possibly any MGC technique and any semiconductor-solvent system. Notably, we would like to mention, that Rogowski et al. are using solvent blends for their coating[15]. Therefore, this model can possibly also be applied to mixed solvent systems, however further verification would be needed to be certain. Moreover Schuettfort et al. grows thin polymer films at the coating speed as predicted by our model[28]. Hence MGC techniques and also our model can likely be employed for other a broad range of material systems as well. Besides,

we should note that in some of the works examined in Fig. 5B, the deviation of experimental speeds from our predicted speeds is likely due to the large steps in the trial and error approach. Smaller step sizes could potentially lead to smaller deviations from the predicted speed and hence to possibly enhanced electrical performance. Lastly, we would like to point out, that the optimal coating speed for heptane at room temperature as predicted by our model is 24.7μm/s, which is very close to the optimal conditions we found with the trial and error method in Fig. 1B. Hence, we believe that our model can successfully replace the trial and error method currently employed in literature and help experimentalist to quickly find the optimum processing speed.

3.4 Optimization using our predictive formula

We prepared single crystalline layers of the organic semiconductor C_8-BTBT with a zone-casting method similar to the setup by Tracz and Pisula[10,11]. The different thermal expansion coefficient between the silicon oxide dielectric and the C_8-BTBT active layer has shown to lead to crack formation at high substrate temperatures[29]. Moreover C_8-BTBT has a phase transition temperature of around 100°C[29,30]. Hence we limited the substrate temperature range to a maximum of 70°C. In order to still ensure reasonable coating speeds, this constrained us to the use of low boiling point solvents only.

In the optimization of the zone-casting of C_8-BTBT films, one is typically moving across a three dimensional parameter space with the solvent, the substrate temperature and the coating speed as axes. Here, we used the model presented in this paper to systematically predict the coating speed for each of the 11 solvent-temperature combinations. We thereby completely remove one of the axes and are left with a much smaller two dimensional parameter space to explore. The electrical quality of the films were evaluated by comparing the averaged characteristics of 50 OTFTs fabricated on each of these layers. As can be seen in Table 1, for each solvent used in this study there exists an optimum substrate temperature. The evolution of the electrical performance with temperature can be non-monotonous, as in the case of heptane. This is likely linked to the complex effects of the substrate temperature on the dynamics on film growth, which is beyond the scope of this study.

Table 1: Fast parameter screening for OTFT optimization with predictive model. OTFT characteristics of C_8-BTBT single-crystalline films prepared with different solvents and substrate temperatures. Each sample is prepared at the best predicted coating speed, enabling fast parameter screening. Device characteristics are averaged over 50 devices on a single sample.

Solvent	Substrate temperature	Coating speed	Device characteristics			
			μ_{eff} (cm^2/Vs)	V_{on} (V)	V_{th} (V)	SS (V/dec)
Hexane	20°C	65 μm/s	3.2±0.4	-4.8±1.4	-13.4±1.6	1.3±0.3
	30°C	99 μm/s	0.3±0.2	-3.2±0.6	-10.4±1.7	1.2±0.4
	50°C	216 μm/s	1E-3±5E-4	-8.0±2.5	-12.4±1.9	3.4±1.5
Heptane	20°C	25 μm/s	3.0±0.4	-4.3±1.1	-12.3±1.3	0.9±0.3
	30°C	39 μm/s	1.1±0.5	-6.3±1.3	-12.3±1.8	0.6±0.2
	50°C	91 μm/s	4.7±0.9	-5.2±1.1	-11.4±1.3	0.4±0.2
	70°C	192 μm/s	2.0±1.2	-6.2±1.3	-11.5±1.5	0.6±0.2
Toluene	20°C	11 μm/s	1.5±0.6	-8.6±1.4	-16.6±2.5	1.3±0.4
	30°C	18 μm/s	4.5±0.8	-6.8±1.4	-16.6±1.8	1.1±0.4
	50°C	43 μm/s	1.5±0.4	-5.7±1.6	-14.0±3.6	1.3±0.4
	70°C	93 μm/s	1.1±0.3	-5.2±1.0	-11.0±2.1	1.3±0.3

The fabrication of C_8-BTBT thin films with heptane at a substrate temperature of 50°C yielded the highest electrical performance. The electrical characteristics depicted in Fig. 6 are well behaved, with a small hysteresis, a high on/off ratio, a low subthreshold slope, and low onset and threshold voltages. We achieved maximum mobilities

surpassing 7 cm^2/Vs with average mobilities of 4.7±0.9 cm^2/Vs over 50 devices. Notably, the mobility is stable over a broad V_g range, indicating a good semiconductor/dielectric interface and no adverse effects from non-linear contact resistances[31,32]. The electrical characteristics are well within the values reported in literature for C_8-BTBT. Hence our model enables a fast parameter screening for the fabrication of any solution processable semiconductor which will yield state of the art electrical results.

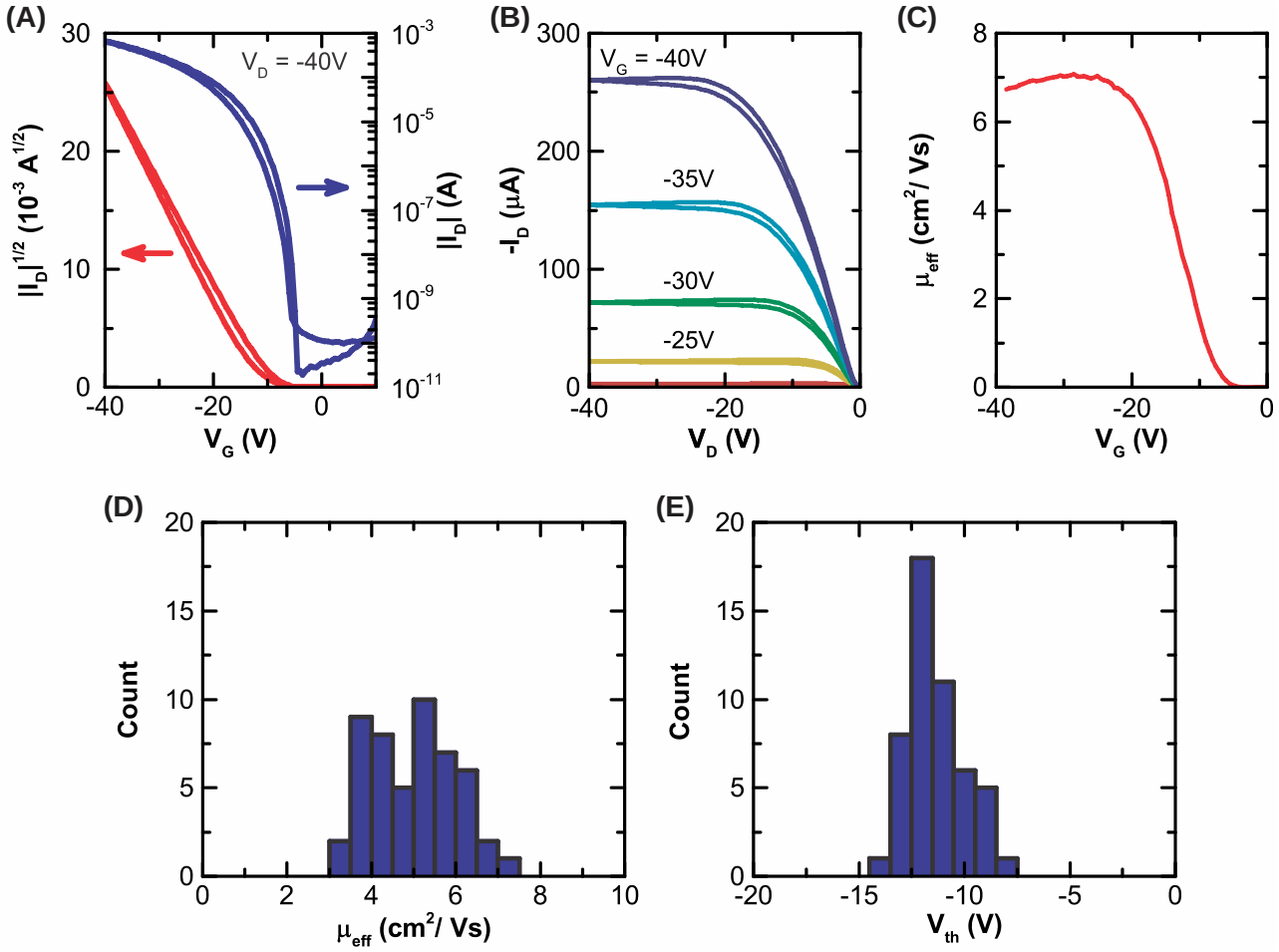

Figure 6: Electrical characteristics of optimized devices. Samples were prepared from a 0.25 wt% C_8-BTBT solution in heptane, zone cast at 50°C at the predicted optimum speed of 91 µm/s. Channel width and length are 1900 µm and 240 µm, respectively. (A) and (B) Transfer and output characteristics[14]. (C) Extracted effective mobility as a function of applied gate voltage[14]. (D) and (E) Statistical variation of effective mobility and threshold voltage of 50 OTFTs measured on the same sample.

4. CONCLUSION

In this work, we develop and validate a predictive model for the optimal coating speed of meniscus guided coating techniques. Our model is further validated by numerical simulations and several results from literature. It can be employed for various fabrication techniques that employ meniscus translation, with virtually any solution processable semiconductor over a wide temperature range and for a broad variety of solvents. Finally, we performed a parameter screening using speeds predicted by this model. This fast and easy optimization route leads to state of the art electrical results, clearly outperforming the current trial and error approach in terms of optimization speed. Hence, our approach greatly facilitates process optimization as it completely removes one important axis from the parameter space to explore.

ACKNOWLEDGEMENTS

This work has supported by the European Research Council under the European Union's Seventh Framework Programme (FP7/2007-2013) / ERC grant agreement nº320680 (EPOS CRYSTALLI) and by the Research Foundation Flanders (FWO Vlaanderen) under the FWO-ARRS research collaboration program / grant number G0B5914N (ORSIC-HIMA). The authors thank Nippon Kayaku Co. for supplying the C_8-BTBT used in the experiments.

REFERENCES

1. Forrest, S. R. The path to ubiquitous and low-cost organic electronic appliances on plastic. *Nature* **428,** 911–918 (2004).
2. Klauk, H. Organic thin-film transistors. *Chem. Soc. Rev.* **39,** 2643–2666 (2010).
3. Sirringhaus, H. 25th anniversary article: Organic field-effect transistors: The path beyond amorphous silicon. *Adv. Mater.* **26,** 1319–1335 (2014).
4. Dong, H., Fu, X., Liu, J., Wang, Z. & Hu, W. 25th Anniversary Article: Key Points for High-Mobility Organic Field-Effect Transistors. *Adv. Mater.* **25,** 6158–6183 (2013).
5. Mei, J., Diao, Y., Appleton, A. L., Fang, L. & Bao, Z. Integrated materials design of organic semiconductors for field-effect transistors. *J. Am. Chem. Soc.* **135,** 6724–6746 (2013).
6. Horowitz, G. & Hajlaoui, M. E. Grain size dependent mobility in polycrystalline organic field-effect transistors. *Synth. Met.* **122,** 185–189 (2001).
7. Lee, S. S. *et al.* Controlling nucleation and crystallization in solution-processed organic semiconductors for thin-film transistors. *Adv. Mater.* **21,** 3605–3609 (2009).
8. Rivnay, J. *et al.* Large modulation of carrier transport by grain-boundary molecular packing and microstructure in organic thin films. *Nat. Mater.* **8,** 952–958 (2009).
9. Wo, S., Headrick, R. L. & Anthony, J. E. Fabrication and characterization of controllable grain boundary arrays in solution-processed small molecule organic semiconductor films. *J. Appl. Phys.* **111,** 073716 (2012).
10. Tracz, A. *et al.* Uniaxial alignment of the columnar super-structure of a hexa (alkyl) hexa-peri-hexabenzocoronene on untreated glass by simple solution processing. *J. Am. Chem. Soc.* **125,** 1682–1683 (2003).
11. Pisula, W. *et al.* A zone-casting technique for device fabrication of field-effect transistors based on discotic hexa-perihexabenzocoronene. *Adv. Mater.* **17,** 684–688 (2005).
12. Duffy, C. M. *et al.* High-mobility aligned pentacene films grown by zone-casting. *Chem. Mater.* **20,** 7252–7259 (2008).
13. Su, Y., Gao, X., Liu, J., Xing, R. & Han, Y. Uniaxial alignment of triisopropylsilylethynyl pentacene via zone-casting technique. *Phys. Chem. Chem. Phys.* **15,** 14396–14404 (2013).
14. Janneck, R., Vercesi, F., Heremans, P., Genoe, J. & Rolin, C. Predictive Model for the Meniscus-Guided Coating of High- Quality Organic Single-Crystalline Thin Films. *Adv. Mater.* (2016). doi:10.1002/adma.201602377
15. Rogowski, R. Z., Dzwilewski, A., Kemerink, M. & Darhuber, A. A. Solution processing of semiconducting organic molecules for tailored charge transport properties. *J. Phys. Chem. C* **115,** 11758–11762 (2011).
16. Jang, J. *et al.* Highly crystalline soluble acene crystal arrays for organic transistors: Mechanism of crystal growth during dip-coating. *Adv. Funct. Mater.* **22,** 1005–1014 (2012).
17. Hofmockel, R. *et al.* High-mobility organic thin-film transistors based on a small-molecule semiconductor deposited in vacuum and by solution shearing. *Org. Electron.* **14,** 3213–3221 (2013).
18. Giri, G. *et al.* Tuning charge transport in solution-sheared organic semiconductors using lattice strain. *Nature* **480,** 504–508 (2011).
19. Diao, Y. *et al.* Solution coating of large-area organic semiconductor thin films with aligned single-crystalline domains. *Nat. Mater.* **12,** 665–671 (2013).
20. Niazi, M. R. *et al.* Contact-induced nucleation in high-performance bottom-contact organic thin film transistors manufactured by large-area compatible solution processing. *Adv. Funct. Mater.* **26,** 2371–2378 (2016).
21. Soeda, J. *et al.* Inch-size solution-processed single-crystalline films of high-mobility organic semiconductors. *Appl. Phys. Express* **6,** 076503 (2013).
22. Smilgies, D. M. *et al.* Look fast: Crystallization of conjugated molecules during solution shearing probed in-situ and in real time by X-ray scattering. *Phys. Status Solidi - Rapid Res. Lett.* **7,** 177–179 (2013).

23. Giri, G. *et al.* One-dimensional self-confinement promotes polymorph selection in large-area organic semiconductor thin films. *Nat. Commun.* **5,** 3573 (2014).
24. Le Berre, M., Chen, Y. & Baigl, D. From convective assembly to landau - Levich deposition of multilayered phospholipid films of controlled thickness. *Langmuir* **25,** 2554–2557 (2009).
25. Uemura, T., Hirose, Y., Uno, M., Takimiya, K. & Takeya, J. Very high mobility in solution-processed organic thin-film transistors of highly ordered [1]benzothieno[32-b]benzothiophene derivatives. *Appl. Phys. Express* **2,** 111501 (2009).
26. Uemura, T. *et al.* Band-like transport in solution-crystallized organic transistors. *Curr. Appl. Phys.* **12,** 87–91 (2012).
27. Soeda, J. *et al.* Solution-crystallized organic field-effect transistors with charge-acceptor layers: High-mobility and low-threshold-voltage operation in air. *Adv. Mater.* **23,** 3309–3314 (2011).
28. Schuettfort, T. *et al.* Microstructure of polycrystalline PBTTT films: Domain mapping and structure formation. *ACS Nano* **6,** 1849–1864 (2012).
29. Fujieda, I., Iizuka, N. & Onishi, Y. Directional solidification of C8-BTBT films induced by temperature gradients and its application for transistors. in *Proceedings of SPIE* **9360,** 936012 (2015).
30. Kwon, S. *et al.* Organic Single-Crystal Semiconductor Films on a Millimeter Domain Scale. *Adv. Mater.* **27,** 6870–6877 (2015).
31. Uemura, T. *et al.* On the Extraction of Charge Carrier Mobility in High-Mobility Organic Transistors. *Adv. Mater.* **28,** 151–155 (2016).
32. Bittle, E. G., Basham, J. I., Jackson, T. N., Jurchescu, O. D. & Gundlach, D. J. Mobility overestimation due to gated contacts in organic field-effect transistors. *Nat. Commun.* **7,** 10908 (2016).